22nd International Conference
ENGINEERING MECHANICS 2016
Svratka, Czech Republic, 9 – 12 May 2016

MORPHOLOGICAL DILATION AS THE METHOD OF MINERAL FRACTION LOSS COMPENSATION IN RECONSTRUCTION OF TRABECULAR BONE STRUCTURE

A. Cichański*, K. Nowicki

Abstract: *The paper presents the issue of compensation of mineral fraction loss during bone reconstruction performed with application of own algorithms. The algorithm of the image morphological dilation was adopted for such compensation. The algorithm efficiency was proved during numerical analyses of bone structures reconstructed with First-Second and First-Last methods for the selected eight sizes of voxels. Application of the image morphological dilation allowed for improvement of the accuracy of structure reconstruction with First-Last method.*

Keywords: ***bone structure reconstruction, finite element method, morphological dilation***

1. Introduction

The content of mineral fraction is decisive for the stiffness of the tested trabecular structure (Topoliński et al. #1, 2012). At the structure modelling stage the voxel size is a significant parameter with respect to stiffness. Decrease of stiffness of the structure modelled with hexahedral elements which accompanies the voxel size increase can be reduced by compensation of the modelled sample volume or by application of tetrahedral elements (Urlich et al., 1998). Other method for stiffness decrease minimization is to apply hexahedral elements for elongated voxels (Topoliński et al. #2, 2012). Application of elements with quadratic interpolation between nodes does not improve accuracy of modelling of the structure resilience properties (Depalle et al., 2013).

Mathematical morphology is vastly applied in processing of medical images. It is mostly used for denoising of images generated with basic methods of medical imagining (Mittal et al., 2013). Morphological filters are also applied in analysis of biological structures, including trabecular bone structures. Skeletal images of trabecular bone structure generated with morphological filters are the basis for determination of structural parameters (Sakoda et al., 2004).

The paper presents the issue of compensation for mineral fraction loss in samples modelled with own structure reconstruction algorithms. The image morphological dilation algorithm was adopted for correction of the structure. Verification of the proposed method for samples of variable structure in the vast range of voxel size variability was performed. During numerical analyses the impact of the proposed compensation method on accuracy of modelling of stiffness of the reconstructed trabecular bone structure was specified.

2. Test object

Modelling was applied to samples of trabecular structure in cylindrical form, of 10mm diameter and 7.5mm height, cut from human femoral neck. Samples preparation method was described in the work by (Topoliński et al. #1, 2012). Trabecular structure samples obtained were subject to μCT80 (Stanco A.G., Switzeland) microtomograph tests. As a result of tests conducted with 36μm resolution, a set of 210 images of layers of structures perpendicular to sample axis were obtained. The images were processed to binary form by thresholding, with threshold value as 18% of maximum brightness of the received image.

* Dr.Eng. Artur Cichański: University of Science and Technology, Mechanical Engineering Faculty, Kaliskiego 7; 85-789, Bydgoszcz; PL, e-mail: artur.cichanski@utp.edu.pl

Three structural models were prepared for each sample: base model SC, model First-Second FS model and First-Last FL model (Topoliński et al. #2, 2012). The models differed in the number of μCT required for their preparation. SC model was based on all images generated with images μCT. FS and FL models were based on the selected μCT images, and the subsequent layers of the reconstructed structure were composed of axially elongated voxels (Fig. 1). During construction of FS models, two subsequent scans, set 36μm apart, were compared. During construction of FL models, two subsequent scans, set total multiple of the base 36μm dimension apart, were compared. For FS and FL models, voxel *d* size varied from 72 to 324μm, with 36μm increment.

a)

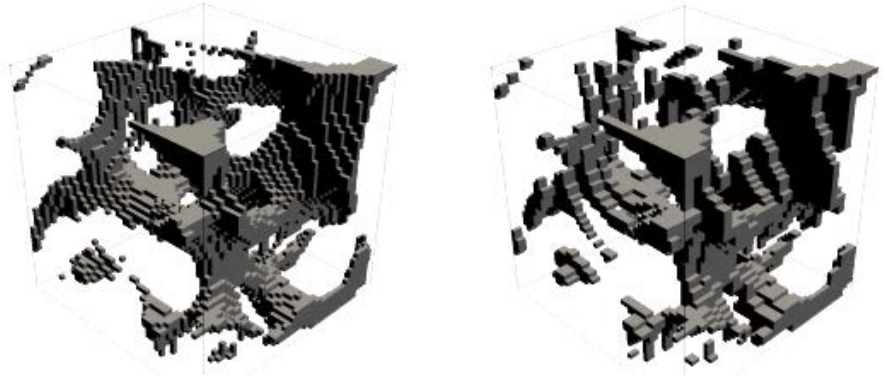

Fig. 1: An example of reconstructed structure: a) SC method; b) FS method, d=108μm.

Application of FS and FL models results in reduction of a number of scans necessary for structure reconstruction, thus it allows for reduction of radiation dose a diagnosed person is exposed to. Mineral fraction loss and the loss of connections between trabeculae in the reconstructed structure and the resulting sample stiffness decrease are undesirable effects of these models . For *BV/TV*=0.353 sample, average volume decrease of models reconstructed with FS method referenced to volumes for SC method is below 1% (Fig 2a), and average Young apparent modulus decrease, referenced to Young apparent modulus for SC method reaches 17% (Fig 2b). For the same sample reconstructed with FL method volume decrease is 43% (Fig 2a), and strength decrease reaches 72% (Fig 2b).

The work uses morphological dilation algorithm for compensation of mineral fraction loss (Gonzalez & Woods, 1992). The applied method realized dilation algorithm with three dimensional structural element 3x3x3 applied for each image in image stack representing individual cross-sections of trabecular bone structure and images in the adjacent stack, above and below the processed image. Dilation algorithm was activated if the original number of pixels representing mineral fraction on the reconstructed image was less than on the unprocessed image. The mask corresponding to actual location of the structural element was placed on the unprocessed image. If the pixels of such mask covered the mineral fraction representing pixels on the unprocessed image, then additional mineral fraction representing pixel was additionally created. As a result of algorithm operation, gradual expansion of edges of the unprocessed image objects and diminishing of openings took place. Such prepared morphological dilation was conducted until the least possible difference in the number of pixels between unprocessed and reconstructed image was reached, upon maintaining lower number of reconstructed image pixels then the number of unprocessed image pixels.

3. Test conditions

For each of three models sample stiffness was specified with finite elements method FEM in ANSYS software environment. The mesh was created with direct voxel to element geometry conversion (Boutroy et al., 2008). Analysis was performed on 8 node SOLID186 elements in the form of cube of side length 36μm. In case of elongated voxels, characteristic for FS and FL methods, several elements were created for the voxel and distributed along its length. Elements not connected with the whole sample structure were eliminated from such prepared mesh. Isotropic material properties E = 10GPa and ν=0.3 were adopted for the analyses. Threshold conditions mapped cylindrical sample compression in axial direction ε=0.8% (Topoliński et al. #2, 2012). Apparent Young modulus for the sample was determined on the basis of the analysis results.

Tab. 1: Selected structural indicators for the modelled samples.

value	*BV/TV*	*Tb.Th* [mm]	*Tb.Sp* [mm]	*Tb.N* [1/mm]
min	0.068	0.76	0.089	0.331
max	0.377	1.956	0.23	1.223
mean	0.224	1.446	0.147	0.612
standard deviation	0.111	0.407	0.044	0.31

Numerical analyses used 9 samples selected from population of 42 samples. As the first the sample of *BV/TV* value closest to *BV/TV* average value for the whole population was selected. Then, 4 samples of *BV/TV* values close to average *BV/TV* plus 0.5, 1, 1.5 and 2 multiple of standard deviation SD for the whole population were selected. The same procedure was applied for subsequent 4 samples for which *BV/TV* value was lower than the average by similar SD multiples. Basic structure indicators specifying the selected samples are presented in Table 1. Significant variability of the indicators and their standard deviations indicates significant variation of the analysed structures. For each selected sample the following calculations were performed: for 1 SC model and 8 FS models without compensation and for 8 FS models with compensation and 8 FL models without compensation and 8 FL models with compensation.

4. Test results

No change was observed for FS method as its characteristic volume decrease was so insignificant that it did not triggered the dilation algorithm. As a result of dilation algorithm application, structure reconstruction error for FL method was reduced. For sample with *BV/TV* =0.353 volume decrease is 20% (FL,CP designation on Fig 2a), Young modulus decrease reaches 48% (FL,CP designation on Fig 2b).

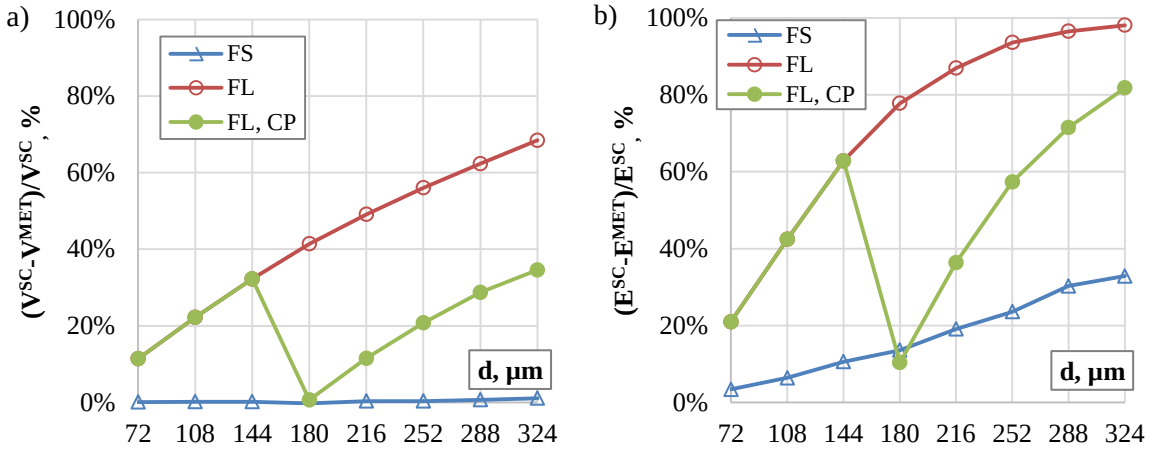

Fig. 2. Structure reconstruction errors for sample BV/TV=0.353, a) volume V; b) apparent modulus E.

Analyses results for 9 samples modelled with FS method and FL method are presented in table 1 for the models without NC compensation and with CP volume compensation. Relative errors of δV^{MOD} volume were calculated from dependency (1) on the basis of FEM analysis results for all eight voxel sizes d changing in the range from 72 to 324µm, with 36µm increment. For the set voxel size d V_d^{SC} volume was determined on the basis of SC model and V_d^{MOD} volume was determined on FS or FL model. Maintaining similar convention of designations, averaged values of relative errors of Young apparent modulus δE were determined.

$$\delta V^{MOD} = \frac{1}{8}\sum_{d=72}^{324} \frac{V_d^{SC} - V_d^{MOD}}{V_d^{SC}} * 100\% \qquad (1)$$

For FS method, values of δV^{FS} volume error and values of δE^{FS} apparent Young modulus error remain unchanged for models with and without compensation. For FL method, application of the image morphological dilation resulted in reduction of δV^{FL} volume error and δE^{FL} apparent Young

modulus error. For both methods, absolute values of δE apparent Young modulus error are higher than the values of δV volume errors. Along with *BV/TV* increase the values of both errors are decreased.

Tab. 1: Reconstruction errors, averaged for all voxel sizes

BV/TV	δV^{FS}		δV^{FL}		δE^{FS}		δE^{FL}	
	NC	CP	NC	CP	NC	CP	NC	CP
0.377	0%	0%	33%	18%	10%	10%	56%	32%
0.353	0%	0%	43%	20%	17%	17%	72%	48%
0.32	0%	0%	46%	18%	18%	18%	72%	45%
0.259	1%	1%	58%	30%	32%	32%	82%	62%
0.217	4%	4%	65%	38%	45%	45%	89%	83%
0.171	9%	9%	69%	52%	52%	52%	90%	85%
0.145	10%	10%	69%	51%	59%	59%	92%	88%
0.107	17%	17%	71%	48%	60%	60%	92%	83%
0.068	31%	31%	74%	53%	70%	70%	95%	90%
mean	**8%**	**8%**	**59%**	**36%**	**40%**	**40%**	**82%**	**68%**

5. Conclusions

FS method maps the modelled structure accordingly. For the samples characterised with high mineral fraction *BV/TV*>0.3 share the method allows for structure reconstruction without volume decrease for voxels of up to 0.3mm length. For this method, the image morphological dilation algorithm was not triggered. The observed decrease of the sample stiffness is influenced by the loss of connections between trabeculae resulting from omission of some μCT images which is characteristic for FS method.

FL method is sensitive to voxel size increase resulting from the increase of distance between μCT images, selected for the structure reconstruction. Even the samples of the highest mineral fraction share modelled with the method show high volume losses. Values of the structure reconstruction errors are comparable to the values obtained for the samples characterised with the lowest mineral fraction share but modelled with FS method.

Application of the image morphological dilation allowed for improvement of the structure reconstruction accuracy with FL method. Average difference between FL and FS models stiffness decreased for all samples. Higher increase of the structure reconstruction efficiency for samples characterized with higher mineral fraction share was observed. For both tested methods, the structure reconstruction accuracy increases with the mineral fraction quantity increase.

References

Boutroy, S., Van Rietbergen, B., Sornay-Rendu, E., Munoz, F., Bouxsein, M. L., Delmas, P. D., 2008, Finite element analysis based on in vivo HR-pQCT images of the distal radius is associated with wrist fracture in postmenopausal women, J Bone Miner Res, 23, 3, pp. 392-399.

Depalle B., Chapurlat R., Walter-Le-Berre H., Bou-Said B., Follet, H. (2013). "Finite element dependence of stress evaluation for human trabecular bone." J Mech Behav Biomed Mater, 18, pp.200-212.

Gonzalez R., Woods R., (1992), Digital Image Processing, Addison-Wesley Publishing Company.

Mittal U., Anand S.,(2013), Effect of morphological filters on medical image segmentation using improved watershed segmentation, Int J of Computer Science & Engineering Technology, 4, 6, pp.631-638

Sakoda S., Kawamata R., Kaneda T., Kashima I., (2004), Application of the digital radiographic bone trabecular structure analysis to the mandible using morphological filter, Oral Science Int, May 2004, pp.45-53

Topoliński T., Cichański A., Mazurkiewicz A., Nowicki K., (2012), Microarchitecture Parameters Describe Bone Structure and Its Strength Better Than BMD, The Scientific World Journal, 2012, Article ID 502781, doi:10.1100/2012/502781, pp.1-7.

Topoliński T., Cichański A., Mazurkiewicz A., Nowicki K., (2012), The Relationship between Trabecular Bone Structure Modeling Methods and the Elastic Modulus as Calculated by FEM, The Scientific World Journal, 2012, Article ID 827196, doi:10.1100/2012/827196, pp.1-9.

Ulrich D., van Rietbergen B., Weinans H., Ruegsegger P., (1998), Finite element analysis of trabecular bone structure: a comparison of image-based meshing techniques, Journal of Biomechanics, 31, 12, pp.1187-1192.